Design of a Printed, Metamaterial-Based Beamformer

Brian B. Tierney and Anthony Grbic
Department of Electrical Engineering and Computer Science,
University of Michigan
Ann Arbor, Michigan, USA
btierney@umich.edu; agrbic@umich.edu

***Abstract* - We report the design of a metamaterial-based antenna beamformer that transforms 7 stipulated inputs to 7 prescribed output beams. The beamformer is printed and exhibits a broad bandwidth of operation. It is modeled as an inhomogeneous, anisotropic 2D medium, and is designed using an constrained optimization approach. This design technique offers improved flexibility and feasibility over coordinate-transformation methods. The constitutive parameters of the beamformer are implemented using printed-circuit metamaterials. Measurement results for the fabricated beamformer are presented and show excellent agreement with the design goals.**

***Index Terms* — Beamformer, finite-element method, metamaterials, optimization, transformation electromagnetics.**

1. Introduction

In this work, we design a printed, metamaterial-based beamformer that radiates a prescribed output beam for each stipulated input excitation, and maintains those beam directions over a wide frequency range. The device is modeled as a 2D inhomogeneous, anisotropic transformation region and realized using tensor transmission-line metamaterials.

Field-transforming metamaterial devices have been designed in recent years using transformation electromagnetics, a technique which exploits the form-invariance of Maxwell's equations under coordinate transformations [1], [2]. However, transformation electromagnetics often yields material parameters that are difficult to implement, such as frequency-dispersive or highly-anisotropic materials. Here, an alternative design procedure is reported that directly searches the material parameter space. The approach combines a custom finite-element method (FEM) forward solver with a constrained optimization algorithm. This approach has two primary advantages over coordinate transformation methods: (1) it constrains material parameters to improve practicality and bandwidth, and (2) it permits the design of devices for which a transformation map is difficult or impossible to define.

2. Design Procedure

The proposed printed-circuit beamformer can be modeled as a 2D inhomogeneous, anisotropic region supporting a vertical electric field polarization ($\vec{E} = E_z\hat{z}$ and $\vec{H} = H_x\hat{x} + H_y\hat{y}$) with material distribution $\epsilon_z(x,y)$ and $\bar{\mu}(x,y)$ (see Fig. 1) [4]. The goal is to find $\epsilon_z(x,y)$ and $\bar{\mu}(x,y)$ that transform the j^{th} stipulated field incident upon the transformation region to the j^{th} prescribed output field, for all j such that $1 \le j \le 7$. The 7 stipulated inputs are modeled as $\hat{z}$-directed line currents, and realized in practice using microstrip feedlines. Each input is positioned 6mm from the input face and spaced at 6mm intervals along x (see Fig. 1). To find the sufficient $\epsilon_z(x,y)$ and $\bar{\mu}(x,y)$, a custom FEM forward solver is coupled to a nonlinear minimization algorithm. The FEM problem is formulated as $\overline{K}\boldsymbol{E_z} = \boldsymbol{b}$, where $\boldsymbol{E_z}$ is a vector containing the E_z values at the vertices of the mesh, $\boldsymbol{b}$ represents the incident field, and $\overline{K}$ is the FEM matrix.

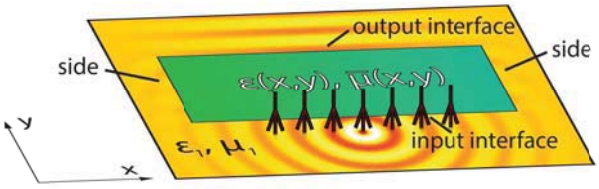

Fig. 1. The beamformer is a 2D inhomogeneous, anisotropic medium of material parameter distribution. The input excitations are modeled as z-directed line currents. The figure shows the center input being excited.

To find the material parameter coefficients $\boldsymbol{g}$ of the beamformer, the following cost function $f(\boldsymbol{g})$ is minimized:

$$f(\boldsymbol{g}) = \sum_{j=1}^{7}\left[1 - \left|\frac{k\left(\boldsymbol{h}_j(x,\boldsymbol{g})\right)\cdot k\left(\boldsymbol{h}_{j0}(x,\boldsymbol{g})\right)^*}{k\left(\boldsymbol{h}_{j0}(x,\boldsymbol{g})\right)\cdot k\left(\boldsymbol{h}_{j0}(x,\boldsymbol{g})\right)^*}\right|^2\right], \quad (1)$$

where the inner product is defined as an integration over the output face of the beamformer/transformation region (see Fig. 1), the subscript j denotes the input number, and the subscript $j0$ denotes the desired distribution for input number j. The function $\boldsymbol{h}_j(x,\boldsymbol{g})$ is

$$\boldsymbol{h}_j(x,\boldsymbol{g}) = \sqrt{P_j(x)}\angle E_{jz}(x), \quad (2)$$

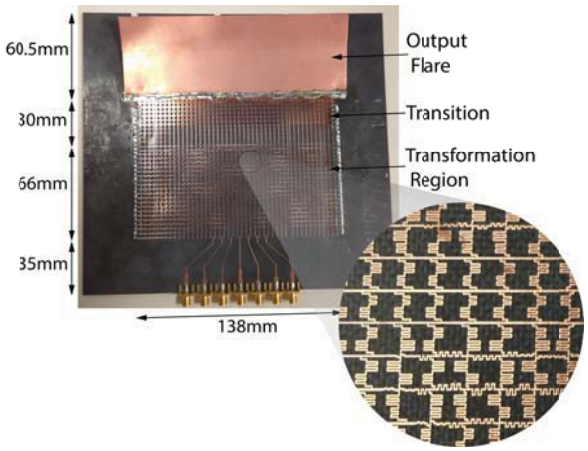

Fig. 2. The fabricated printed-circuit antenna beamformer prototype. A flare antenna is soldered to the output of the beamformer to transition the guided waves on the beamformer to radiated waves. Surface mount resistors are soldered to the sides of the beamformer to prevent reflections within the transformation region.

where $P_j(x)$ is the total power density and $\angle E_{jz}(x)$ is the phase of the electric field at a point x along the output interface. The variable k represents a function that emphasizes the shape of the output field distribution over the total power:

$$k\left(\boldsymbol{h}_j(x,\boldsymbol{g})\right) = \boldsymbol{h}_j(x,g)\cdot\min\left\{1,\frac{\left|\boldsymbol{h}_{j0}(x,\boldsymbol{g})\right|}{\left|\boldsymbol{h}_j(x,\boldsymbol{g})\right|}\right\}. \qquad (3)$$

In order to minimize $f(\boldsymbol{g})$ subject to the constraints on the material parameters, the active-set algorithm [5] is employed and implemented using MATLAB.

3. Beamformer Design

Using the procedure outlined in Section 2, the beamformer was designed. The device is similar to the one presented in [4], except that it is designed for 7 input/output combinations, rather than a single input/output pair. The design frequency of the beamformer is 10 GHz. The beamformer itself consists unit cells that are d = 3mm in dimension. The permittivity of the beamformer is fixed at $\epsilon_z(x,y)=\epsilon_0$, while the eigenvalues of the permeability tensor are bounded below by $2.96\mu_0$ and above by $8.88\mu_0$. The medium surrounding the transformation region/beamformer has the same unit cell dimension, and is chosen to have $\epsilon_{z1}=\epsilon_0$ and $\mu_1=2.96\mu_0$. The prescribed output beam angles associated with the 7 stipulated inputs are set to (-30°, -20°, -10°, 0°, 10°, 20°, 30°).

After finding $\bar{\mu}(x,y)$, the printed-circuit implementation is designed using a procedure similar to that reported in [4]. The fabricated beamformer is shown in Fig. 2. The substrate is Rogers RT/Duroid 5880 with dielectric thickness of 31mil. The sides of the transformation region are terminated in surface-mount resistors. An flare antenna is soldered to the output of the beamformer to transition the guided waves on the beamformer to radiated waves. Transmission-line matching networks are designed at each input feedline.

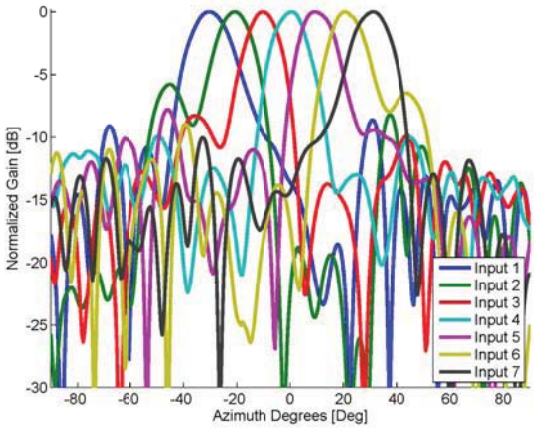

Fig. 3. Measured co-polarized, azimuthal (H-plane) far-field patterns at 10 GHz. The measurements show good agreement with the prescribed design goals.

Fig. 3 provides the measured azimuthal far-field patterns at 10 GHz for each of the 7 inputs. Between 10 GHz and 13 GHz, the measured azimuthal angles of radiation match the prescribed values within $\pm 2°$. The simulated radiation efficiency is between 30% to 43% for each input/frequency pair.

4. Conclusion

A compact, broadband, printed-circuit beamformer was designed and measured. The device transforms 7 stipulated inputs to 7 prescribed output beams. The design procedure employs a custom FEM solver coupled to a nonlinear optimization algorithm. The efficient design technique has two primary advantages over transformation electromagnetics, (1) the ability to constrain material parameters in order to improve practicality and bandwidth, and (2) the ability to design devices for which a transformation map may be difficult or impossible to define. Measurement results show good agreement with the design goals of the beamformer.

Acknowledgment

This work was supported by the National Reconnaissance Office (NRO) under NRO grant NRO000-15-C-0048.

References

[1] J. B. Pendry, D. Schurig, and D. R. Smith, "Controlling electromagnetic fields," *Science*, vol. 312, no. 5781, pp. 1780-1782, 2006.

[2] U. Leonhardt, "Optical conformal mapping". *Science,* vol. 312, no. 5781, pp. 1777-1780, 2006.

[3] D. H. Kwon and D. H. Werner, "Transformation electromagnetics: an overview of the theory and applications," *Antennas and Propagation Magazine, IEEE,* vol. 52, no. 1, pp. 24-46, 2010.

[4] G. Gok and A. Grbic, "A printed antenna beam former implemented using tensor transmission-line metamaterials," in *Antennas and Propagation Society International Symposium (APSURSI),* 2014 IEEE, July 2014, pp. 765-766.

[5] J. Nocedal and S. Wright, *Numerical Optimization.* Springer Science & Business Media, 2006.